scientific reports

Check for updates

OPEN

Facilitating DNAzyme transport across the blood-brain barrier with nanoliposome technology

Mohammad Javad Hoseinifar[1,8], Faranak Aghaz[1,7]✉, Zahra Asadi[2,3,8], Peyman Asadi[1], Seyed Ershad Nedaei[4], Elham Arkan[1], Ali Pourmotabbed[4], Gholamreza Bahrami[5] & Tayebeh Pourmotabbed[6]✉

Recently, oligonucleotide post-transcriptional gene silencing, antisense oligonucleotides, small interfering RNA, ribozymes, and Deoxyribozymes (DNAzymes) have been used to tackle neurodegenerative diseases such as Alzheimer's and polyglutamine diseases like Huntington's disease. However, the primary obstacle to the therapeutic effectiveness of these oligonucleotides is the blood-brain barrier (BBB), a crucial protective mechanism limiting drug penetration into brain cells. In this study, we generated a DNAzyme-loaded nanoliposome (DNZ-NLP) as a drug delivery system to effectively deliver and release the DNAzymes to the brain. The investigation of physicochemical characteristics of fabricated nanoliposomes, particularly size, morphology, and surface charge, revealed that the size of DNZ-NLPs was ~68 nm, an optimum size for brain delivery. Cellular uptake and cytocompatibility studies using SH-SY5Y human neuroblastoma cells demonstrated that both blank nanoliposomes (B-NLPs) and DNZ-NLPs were cytocompatible, and DNZ-NLPs had a stable biphasic release profile in 48 h. Most importantly, about 60% of intravenously administered DNZ-NLPs to the healthy mouse were found in the brains of the animals. These findings confirmed that DNZ-NLPs passed the BBB. The controlled release of DNAzymes, the maximal cytocompatibility, and significantly improved BBB permeability suggest that our DNZ-NLPs offer a promising formulation for delivering all types of oligonucleotides to the brain for neurodegenerative disease treatments.

Keywords DNAzyme, Blood-Brain barrier, Nanoliposome, BBB permeability

The presence of the blood-brain barrier (BBB), a tightly interconnected network of blood vessels and endothelial cells that restricts the entry of foreign particles larger than 100 nm into the brain, poses considerable challenges and complexities in advancing therapeutic strategies for neurodegenerative diseases (NDs)[1]. Due to inadequate early detection of these ailments and lack of effective therapies, they have become the leading life-threatening health burden globally compared to other major illnesses, and they have had a terrible negative impact on public health[2]. On the other hand, traditional drug delivery methods are ineffective for treating NDs due to the limitations imposed by the BBB. This barrier is the main obstacle to passing the appropriate drug concentration and has presented us with numerous challenges[3]. In recent years, researchers have concentrated on innovative brain drug delivery systems less than 100 nm, to overcome these complications[4].

Gene therapies, specifically DNAzymes, post-transcriptional gene silencing technique, have shown promising results in treating neurodegenerative diseases[5]. DNAzymes are single-stranded DNA-based catalytic molecules functioning as efficient RNA-silencing agents; they target, bind to, and degrade disease-associated mRNAs, reducing the levels of proteins implicated in specific pathological conditions[6]. A 10–23 DNAzyme possesses a central catalytic domain composed of a defined sequence of 15 deoxynucleotides, conferring RNA endonuclease activity. Additionally, this molecule contains two domains that can be designed to hybridize the DNAzyme

[1]Nano Drug Delivery Research Center, Faculty of Pharmacy, Kermanshah University of Medical Sciences, Kermanshah, Iran. [2]Students Research Committee, Kermanshah University of Medical Sciences, Kermanshah, Iran. [3]Department of Clinical Biochemistry, School of Medicine, Kermanshah University of Medical Sciences, Kermanshah, Iran. [4]Department of Physiology, School of Medicine, Kermanshah University of Medical Sciences, Kermanshah, Iran. [5]Medical Biology Research Center, Health Technology Institute, Kermanshah University of Medical Sciences, Kermanshah, Iran. [6]Department of Microbiology, Immunology, and Biochemistry, Health Science Center, University of Tennessee, Memphis, TN, USA. [7]Nano Drug Delivery Research Center, Faculty of Pharmacy, Health Technology Institute, Kermanshah University of Medical Sciences, Kermanshah, Iran. [8]Mohammad Javad Hoseinifar and Zahra Asadi: These authors contributed equally to this work ✉email: Faranak_aghaz@yahoo.com; tpourmot@uthsc.edu

precisely to a target mRNA[7]. It offers a promising approach for designing allele-specific DNAzymes capable of selectively targeting mutant mRNA rather than the wild type[8]. Moreover, DNAzymes present advantages over RNAi-based therapies and antisense oligonucleotides (ASOs) in the aspects of dose-dependent efficacy, catalytic efficiency, stability, and safety[9,10]. DNAzymes have demonstrated well-tolerability in clinical trials targeting c-jun and EBV LMP1 proteins, because these molecules can cross the BBB following systemic injection, eliminating the need for direct brain injections[11]. Thus, DNAzymes hold the potential as an alternative to existing treatments for neurodegenerative diseases[12]. However, their limited ability to cross the BBB (under 6%) hinders routine formulations from achieving therapeutic concentrations in the brain, significantly restricting their clinical applicability[13]. Therefore, employing an efficient drug delivery system is vital to minimize these limitations and improve the therapeutic efficacy of DNAzymes.

To address these challenges, nanotechnology offers the potential to enhance BBB permeability by using bioengineered nanocarriers designed to interact at the cellular level in living organisms[14]. Among the diverse nanocarriers developed for central nervous system (CNS) delivery, lipid nanoparticles, including solid lipid nanoparticles (SLNs), nanoliposomes, nanoemulsions, and nanostructured lipid carriers (NLCs), are regarded as the most promising drug delivery systems. This is due to their efficacy in encapsulation, ability to traverse biological membranes, capacity for transporting lipophilic drugs, low cytotoxicity, and suitable size, as highlighted by research findings[15–21]. Specifically, nanoliposomes have gained attention as a drug delivery system that has the potential to deliver drugs to the specific target sites of the brain after passing the BBB effectively, using particular pathways[22–24].

Thus, the study aimed to synthesize nanoliposomes from soy lecithin using the ethanol injection method, serving as carriers to deliver DNAzymes for targeted brain modification and enhancing their ability to cross the BBB by more than 6%. To this end, after synthesizing and investigating the physicochemical properties of DNAzyme-loaded nanoliposomes (DNZ-NLPs), both in vitro and in vivo studies were performed using SH-SY5Y brain cells and BALB/c mice, respectively. A schematic representation of the present study is shown in Fig. 1.

Materials and methods

Materials

A DNAzyme against the Huntintin gene was designed following the guidelines published by Santoro and Joyce (Santoro SW, Joyce GF. A general purpose RNA-cleaving DNA enzyme. Proc Natl Acad Sci USA 1997;94:4262–4266) and was purchased from Bioneer Company (South Korea). Soybean L-a-Lecithin, fetal bovine serum (FBS), Phosphate buffered solution (PBS), MTT kit (3-(4, 5-dimethylthiazol-2-yl)-2, 5-diphenyltetrazolium

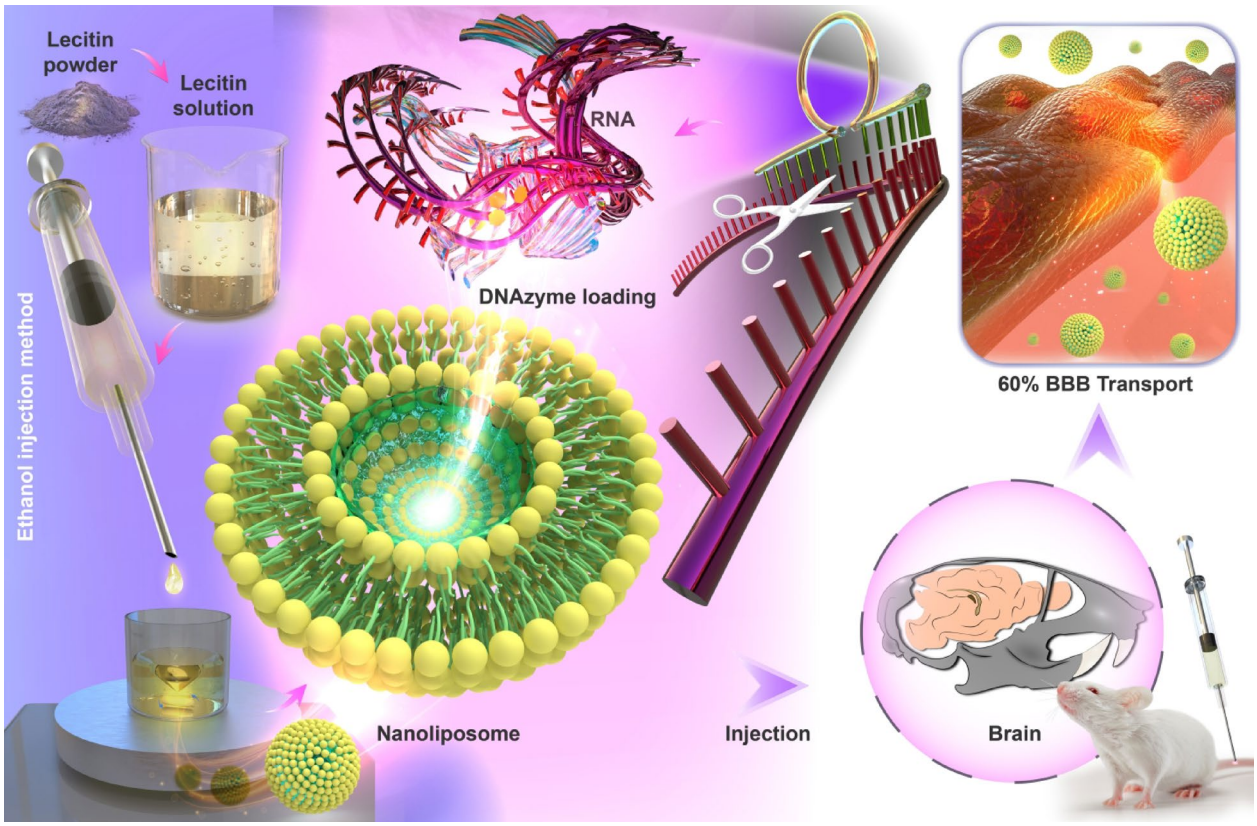

Fig. 1. Enhance the capability of DNZ-NLPs in crossing the BBB to 60%.

bromide), Ethanol (ACS reagent, ≥ 99.5%) and the other additional chemicals and solvents were obtained from Sigma Aldrich (St. Louis, MO, USA) and were used in analytical grades.

Preparation of nanoliposomes and drug loading

Preparation of DNZ-NLPs was performed by optimizing an ethanol injection method[25]. A solution containing 1 mg/mL of lecithin was prepared using pure ethanol. Meanwhile, 20 µg DNAzymes were slowly dissolved in 20 mL of ultrapure water. The lipid/ethanol solution (4 ml) was then slowly added one drop per 5 s to the DNAzymes solution under intense stirring (1300 rpm), using a Hamilton syringe, for greater control and accuracy. Then the resulting mixture was kept under a vigorous stirrer at intense stirring (1300 rpm, 25 °C) and evaporation until about 1.5 ml of DNZ-NLPs was recovered. Finally, sonication was performed using the ultra-probe system (UW2070, BANDELIN electronic Co., Germany), in two 15-second intervals with a 10-second rest period between them at 100 W and cycle 9, to reduce the nanoparticles' size. The blank nanoliposomes (B-NLPs) were fabricated using the same protocol without applying DNAzymes.

Basic physicochemical properties of DNZ-NLPs

The polydispersity index (PDI), particle size, and particle surface charge (zeta potential) of B-NLPs and DNZ-NLPs were determined through the dynamic light scattering (DLS) technique, utilizing the Zetasizer instrument (Malvern Instruments Ltd., Worcestershire, UK) at 25 °C. In addition, essential properties, including aggregation, particle size, morphology, and shape of both B-NLPs and DNZ-NLPs, were analyzed using scanning electron microscopy (SEM) (EM3200, KYKY Technology Co., China) operated at 25 kV, after being coated with gold-palladium membranes[26] .

Determination of drug loading (DL (%)) and entrapment efficiency (EE (%)) of DNZ-NLPs

To evaluate the DNAzymes loading and the entrapment efficiency of DNZ-NLPs, the concentration of DNAzymes in nanoliposomes was measured at 260 nm using a standard curve obtained from known concentrations of pure DNAzyme solutions[27]. For this purpose, freshly prepared DNZ-NLP nanoliposome suspension was centrifuged at 14,800 rpm and 25 °C for 30 min. The concentration of free DNAzymes in the supernatant was determined at 260 nm. The DL (%) and EE (%) values were calculated using the following formula:

$$\mathrm{DL}\ \% = \frac{\text{Total DNAzymes} - \text{Free DNAzymes}}{\text{Loaded DNAzymes} + \text{ Nanoliposome Weight}} \times 100$$

$$\mathrm{EE}\ \% = \frac{\text{Total DNAzymes} - \text{Free DNAzymes}}{\text{Total DNAzymes}} \times 100$$

Fourier transform infrared spectroscopy (FTIR)

An IR Prestige-21 FTIR spectrophotometer (Shimadzu Co., Japan) was employed to analyze the FTIR spectra of pure DNAzymes, B-NLPs, and DNZ-NLPs. At first, 1–2 mg of DNAzymes, B-NLPs, and DNZ-NLPs were separately mixed with spectroscopy-grade KBr pellets, and the resulting mixture was placed in the sample holder of the FTIR device. Finally, the spectra were obtained at room temperature in the 400–4000 cm^{-1} range and at 4 cm^{-1} resolution[28].

In vitro drug release

The rate of release of DNAzymes from DNZ-LNPs was quantitatively measured by the dialysis method as previously described[29]. Briefly, 2 mL of freshly synthesized DNZ-LNPs nanoformulation was placed into a dialysis membrane and incubated against 25 mL PBS for 48 h at 37 °C under stirring (100 rpm). 750 µL of the incubated media was removed at different time intervals (0, 1, 2, 3, 4, 5, 8, 12, 15, 32, 40, 42, 44, 46, and 48 h), and was equivalently replaced with fresh PBS. At the end, the collected media were analyzed for DNAzyme concentration by measuring their absorbance at 260 nm, and the drug release percentage was calculated. All the samples were measured in triplicate[30].

In vitro cell culture model

SH-SY5Y (CRL2266, Sigma-Aldrich Chemical Co., St. Louis, USA) cells were cultured in DMEM/F12 growth medium (Gibco, USA) supplemented with FBS (10% v/v) and antibiotic solution (100 U/mL penicillin, 100 µg/mL streptomycin) and incubated at 37 °C in a humidified chamber with 5% CO2 [31]. The culture media were replaced every 48 h.

Cytocompatibility assay

The cytocompatibility of DNZ-NLPs against SH-SY5Y cells was determined using the MTT assay. SH-SY5Y cells were seeded in 96-well plates at a density of ~ 5000/ per well, and they were exposed to various concentrations (10, 25, 50, 100, and 200 µg/mL) of DNZ-NLPs for 24 h. After this time, the culture medium was discarded, cells were washed with PBS, and incubated with MTT solution (5 mg/mL) in the dark at 37 °C and 5% CO_2 for 4 h. To eliminate formazan crystals, 200 µLof DMSO was then replaced with the media, and absorbance values were measured at 570 nm, using a spectrophotometric Plate Reader (ELx808, Lonza Biotech Co., Switzerland). The percentages of Cell viability and IC_{50} values were calculated using the equation below[32]:

$$\text{Cell viability}\ (\%) = \frac{\text{OD 570 (test)}}{\text{OD 570 (control)}} \times 100$$

Intracellular uptake and in vitro stability

To assess DNZ-NLP cellular uptake and stability, SH-SY5Y cells were transfected with fluorescein isothiocyanate (FITC)-labeled DNAzyme and FITC-labeled DNZ-NLPs. Initially, 5 mg/mL suspension of DNZ-NLPs was added gradually to an equal volume of FITC (5 µg/mL) and was then placed on the stirrer for 12 h at room temperature. The resulting mixture was then centrifuged for 10 min at 10,000 rpm and washed three times with PBS[33]. FITC-labeled DNAzyme was prepared using the same protocol. SH-SY5Y cells were seeded in a six-well culture plate at a density of 1×10^3 cells per well and then incubated overnight at 37 °C. The cells were then washed with PBS three times and incubated with 500 µl FITC-labeled DNZ-NLPs and FITC-labeled DNAzyme with a final concentration of 200 µg/mL at 37 °C for 4 h. The cells were then washed with PBS, fixed in 4% paraformaldehyde (100 µL/well), and nuclei were stained with 40 µM of 4′, 6-diamidino-2-phenylindole (DAPI). Finally, the intracellular uptake of nanoliposomes was assessed using a Cytation cell imaging system (Cytation 5, Biotech Co., USA)[34].

BBB permeability

Female BALB/c mice ($n = 10$) were purchased from the Laboratory Animal Center at the Iran Pasteur Institute (Karaj, Iran). All animal experiments were performed following approval by the Kermanshah University of Medical Sciences Institutional Animal Care and Use Committee (IACUC), and all methods were conducted under the relevant guidelines and regulations. The mice were kept in a state of well-being in an environment that adhered to ethical standards, with unrestricted access to the standard diet, following a 12-hour light-dark cycle.

To evaluate the ability of DNZ-NLPs to pass through the BBB,10 female BALB/c mice (4–6 weeks of age) were injected with FITC-labeled free DNAzymes and FITC-labeled DNZ-NLPs (1 µg/kg) via the tail vein. Animals were then sacrificed at 4 h ($n = 5$) and 24 h ($n = 5$) post-treatment with CO_2 asphyxiation. Then the mouse brains were dissected and fixed in formalin, and 50-µm-thick sections were prepared. The brain slices were then visualized under a fluorescent microscope (Olympus, Tokyo, Japan). The percentage of penetrated free-DNAzymes and DNZ-NLPs to the BBB was calculated using the total area of the section of interest, accounting for the area occupied by fluorescent emitting particles, and utilizing the following formula:

$$\text{Penetration}(\%) = \frac{Area\ occupied\ by\ fluorescent\ emitting\ particles}{Total\ area\ of\ the\ section} \times 100$$

Statistical analysis

The data were analyzed using GraphPad Prism software (version 10.0 for Windows). Statistical judgment between groups was performed using a one-way ANOVA test. A P-value of ≤ 0.05 for all analyses was considered statistically significant.

Results

Physicochemical analysis

Table 1 indicates the physicochemical properties of fabricated nanoparticles. Based on DLS measurements, the B-NLPs were relatively homogeneous with moderate size variability (76.34 nm, PDI = 0.219; Fig. 2, A). Loading DNAzymes into B-NLPs resulted in a slight increase in size distribution, with a Z-average size of 91.49 nm and PDI of 0.325 (Fig. 2, C), indicating that the encapsulation process led to a slightly larger particle size compared to the nanoliposome formulation. The zeta potential analysis indicated − 8.42 mV for B-NLPs at pH 7.4 (Fig. 2, B). Subsequently, upon loading with DNAzymes, the zeta potential of DNZ-NLPs dropped to -12.6 mV (Fig. 2, D). The SEM analysis revealed a uniform distribution of DNZ-NLPs without aggregation, showcasing a spherical shape with an average diameter of approximately 68 nm (Fig. 3). The amount of EE (%) in single DNZ-NLPs was 38%. The DNAzymes were loaded in the nanoliposomes, with a DL (%) of approximately 40%. The data presented in this study demonstrate the successful fabrication of DNZ-NLPs with a spherical morphology and a narrow size distribution.

FTIR

The formation of DNZ-NLPs was evaluated by FTIR (Fig. 4). The FTIR spectrum of DNAzymes suggests a complex mixture of functional groups. The presence of O-H/N-H stretching around 3418 cm^{-1} indicates alcohol, phenol, or amine functionalities. The peaks at 2922 cm^{-1} and 1643 cm^{-1} suggest the presence of aliphatic C-H bonds and C = C bonds, indicating alkanes and unsaturated compounds. Notably, the peak at 1663 cm^{-1} may indicate conjugated alkene systems or allenes, which further supports unsaturation in the structure. Additionally, the presence of C-N stretching at 1238 cm^{-1} indicates nitrogen-containing functional groups, such as amines or amides, while the C-O stretching at 1059 cm^{-1} suggests the presence of alcohols, ethers, or esters.

-	Z-Average (nm)	Zeta potential (mV)	PDI	DL (%)	EE (%)
B-NLPs	76.34	-8.42	0.219	-	-
DNZ-NLPs	91.49	-12.6	0.325	40	38

Table 1. Physicochemical characteristics of B-NLPs and DNZ-NLPs.

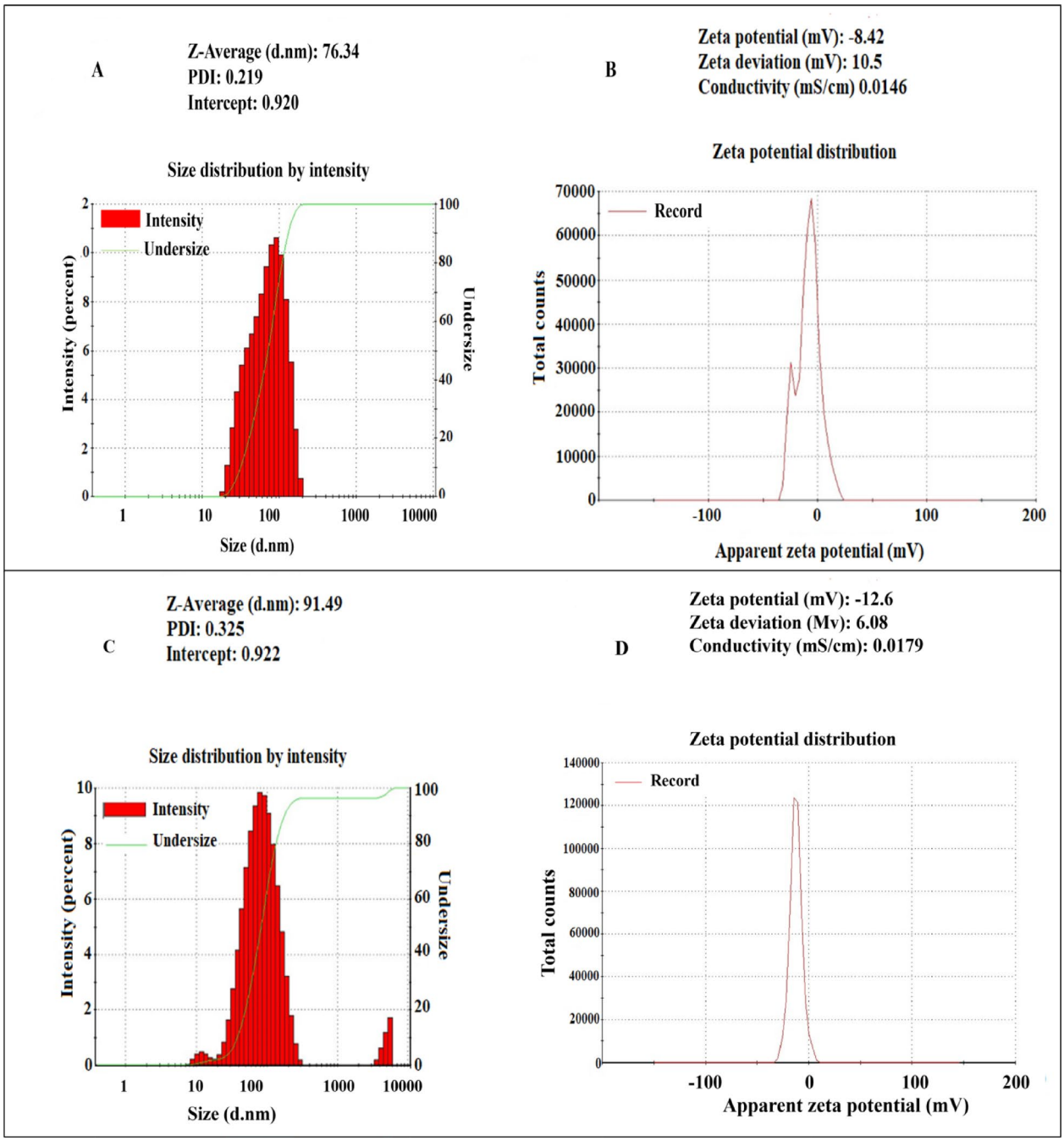

Fig. 2. Size distribution of (**A**) B-NLPs with the size of 76.34 and PDI of 0.219 and (**B**) DNZ-NLPs with the size of 91.49 and PDI of 0.325. The zeta potential measurements demonstrate that (**C**) B-NLPs have a zeta potential of -8.42 mV, while (**D**) DNZ-NLPs exhibit a zeta potential of -12.9 mV.

The B-NLP FTIR spectrum shows several characteristic absorption bands that suggest a complex organic compound with various functional groups. The broad peak around 3397 cm^{-1} indicates the presence of O-H or N-H groups, implying hydroxyl or amine functionalities. The peaks at 2918 cm^{-1} and 2855 cm^{-1} indicate the presence of aliphatic C-H stretching, suggesting the presence of saturated hydrocarbon chains. A strong peak at 1730 cm^{-1} reveals the presence of ester functional groups due to the C = O stretching vibration. The peak at 1670 cm^{-1} suggests unsaturation in the compound, possibly from alkenes or conjugated systems. Additionally, the presence of C-N stretching at 1504 cm^{-1} and 1238 cm^{-1} indicates nitrogen-containing functional groups, such as amines or amides, while the peak at 1080 cm^{-1} suggests C-O bonds, potentially from esters or alcohols.

The successful loading of DNAzymes into nanoliposomes was confirmed by comparing the characteristic peaks of B-NLPs, DNAzymes, and DNZ-NLPs. The broad absorption band observed at 3418 cm^{-1} in DNAzymes, corresponding to N-H and O-H stretching vibrations, was retained in the DNZ-NLPs spectrum at 3408 cm^{-1}, indicating the presence of DNAzymes within the nanoliosomes. Additionally, the ester C = O stretching peak at

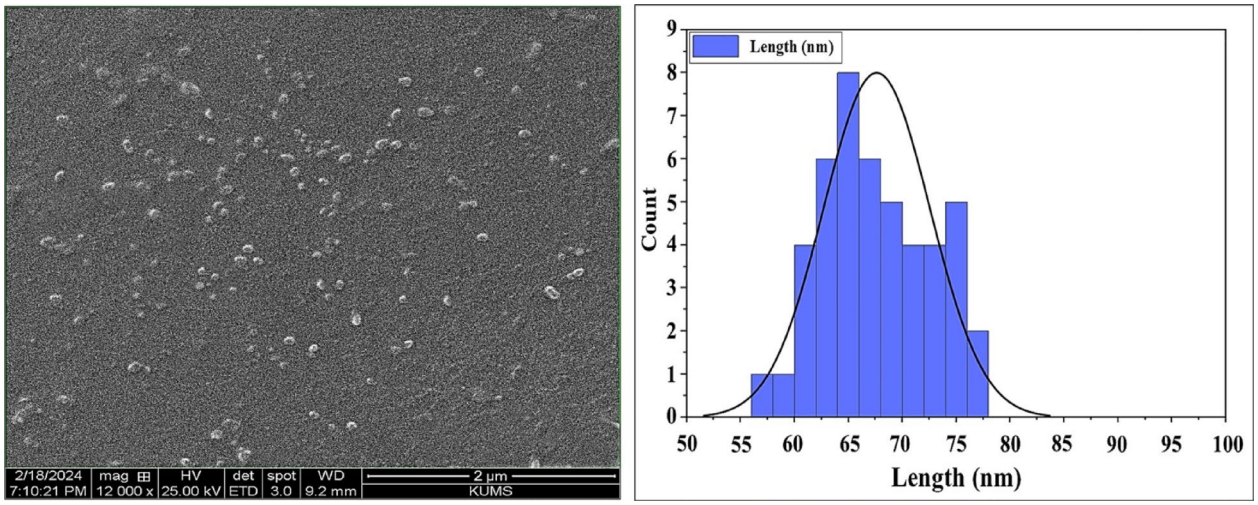

Fig. 3. SEM analysis of DNZ-NLPs with morphologically uniform particles averaging 68 nm in diameter at a scale of 2 µm.

1730 cm^{-1} in nanoliposomes shifted to 1728 cm^{-1} in DNZ-NLPs, suggesting interactions between DNAzymes and the nanoliposomes` matrix. The alkene C = C stretching vibration, which appeared at 1643 cm^{-1} in DNAzymes, shifted to 1663 cm^{-1} in DNZ-NLPs, further confirming the incorporation of DNAzymes. Furthermore, characteristic C-N and C-O stretching vibrations at 1238 cm^{-1} and 1080 cm^{-1} were retained in the DNZ-NLPs spectrum, reinforcing the successful encapsulation. These spectral changes indicate the effective loading of DNAzymes into nanoliosomes while maintaining the structural integrity of both components, confirming the potential of nanoliosomes as a delivery system for DNAzymes.

Kinetic and in vitro drug release

The release kinetics of DNAzymes was analyzed using various mathematical models, including first-order kinetics ($R^2 = 0.93$, Fig. 5, A), Korsmeyer-Peppas ($R^2 = 0.99$, Fig. 5, B), Zero-order kinetics ($R^2 = 0.90$, Fig. 5, C), Hixson-Crowell ($R^2 = 0.91$, Fig. 5, D), and Higuchi ($R^2 = 0.98$, Fig. 5, E). The R^2 of all the mathematical models is high in the range of 0.90–0.99, indicating that the data is order kinetics. And suggests that the models explain a large portion of the variability in our data, which is a strong indicator of good model performance. Based on a dialysis experiment, the cumulative percentage of drug release was monitored over time, and the data were fitted to these kinetic models. Among the tested models, Korsmeyer-Peppas exhibited the highest coefficient of determination ($R^2 = 0.99$), indicating a good correlation between the observed and predicted values (Fig. 5, B). Therefore, the release of DNAzymes from the formulation was found to follow Korsmeyer-Peppas kinetics, suggesting an anomalous (non-Fickian) diffusion release mechanism. The Korsmeyer-Peppas model is a widely used mathematical model that describes the release of drugs from nanocarrier systems, particularly in the context of controlled release formulations. It provides insight into the mechanism of drug release and can characterize different release behaviors based on the type of carriers and drug formulation.

The in vitro release of DNAzymes from DNZ-NLPs was examined by the dialysis bag method at pH 7.4 and for up to 48 h (Fig. 6). The first part of the in vitro release graph suggests two rates, a fast release (from time zero to 10 h) and a slow release (from about 15 to 48 h). These rates were calculated from the slope of the lines drawn through the graph from 0 to 10 h (fast-release, 4.3% of DNAzymes released/hour) and from 10 to 48 h (slow release, 0.2% of DNAzymes released/hour).

Moreover, no significant drug release was observed at the beginning, indicating the stability of the DNZ-NLPs. However, an initial burst release of 36.38% was detected after 1.5 h. The cumulative drug release gradually increased over time, with sustained drug release observed at 2 h (40.88%) and 3 h (45.37%). The release rate remained stable until 15 h. The release rate continued to rise, reaching 49.86% at 32 h. From 32 to 48 h, the release percentage remained stable without any fluctuations. The sustained release behavior indicates the ability of nanoliposomes to maintain drug concentration within a therapeutic range over an extended period.

In vitro cell culture model

Cytocompatibility/safety of DNZ-NLP

The cytocompatibility effects of DNZ-NLPs (at concentrations of 10, 25, 50, 100, and 200 µg/mL) were assessed against SH-SY5Y cells. As shown in Fig. 7, DNZ-NLPs up to 200 µg/mL tested had a minimal impact on SH-SY5Y viability, highlighting the potential safety of DNZ-NLPs as an effective formulation for treating neurodegenerative disease.

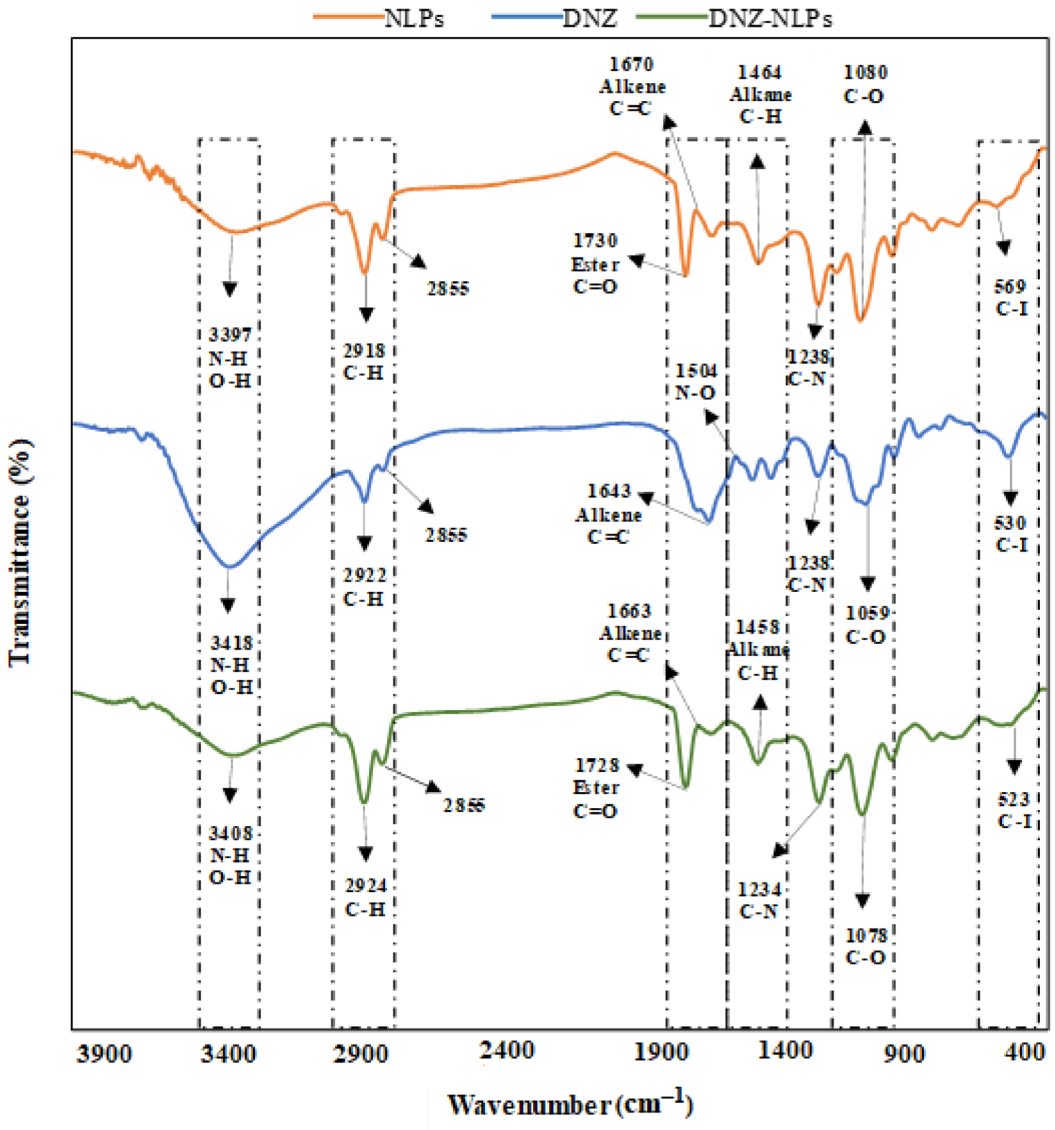

Fig. 4. FTIR spectra of DNAzymes, B-NLPs, and DNZ-NLPs in the 400–4000 cm^{-1} range and at 4 cm^{-1} resolution.

Intracellular uptake and in vivo stability of DNZ-NLP

For investigating cellular uptake and stability, SH-SY5Y cells were cultured and transfected with FITC-labeled DNZ-NLPs and FITC-labeled DNAzyme with a final concentration of 200 µg/mL. At 4 h post-transfection, cells were visualized by confocal microscopy (Fig. 8). The nucleus was visualized by DAPI/anti-fade. As shown in Fig. 8, A, bright green signals corresponding to FITC-labeled DNZ-NLP molecules are present in cells for at least 4 h post-transfection and are located in both the cytosol and the nucleus. Merging the DAPI and FITC channels illustrates the spatial relationship between FITC-labeled components and cell nuclei. The merged image demonstrates partial overlap of FITC fluorescence with nuclear regions, suggesting possible nuclear or perinuclear targeting of the labeled molecule. The nucleus localization significantly increases the effectiveness of DNAzyme therapy.

In vivo model

BBB permeability

The BBB permeability and the distribution of DNZ-NLPs within brain tissues were examined by intravenously injecting female BALB/c mice with fluorescently labeled free-DNAzymes and DNZ-NLP. The animals were sacrificed at 4 and 24 h (Fig. 9) post-DNZ-NLP injection, and their brains were harvested, sectioned, and viewed under a fluorescent microscope. As shown in Fig. 9, A, fluorescently labeled free-DNAzymes could rarely appear inside the brain in a diffuse pattern within the brain parenchyma for up to 4 and 24 h, indicating that DNZ-NLP passes the BBB but at a lower rate. While green fluorescence (Fig. 9, A) revealed that FITC-

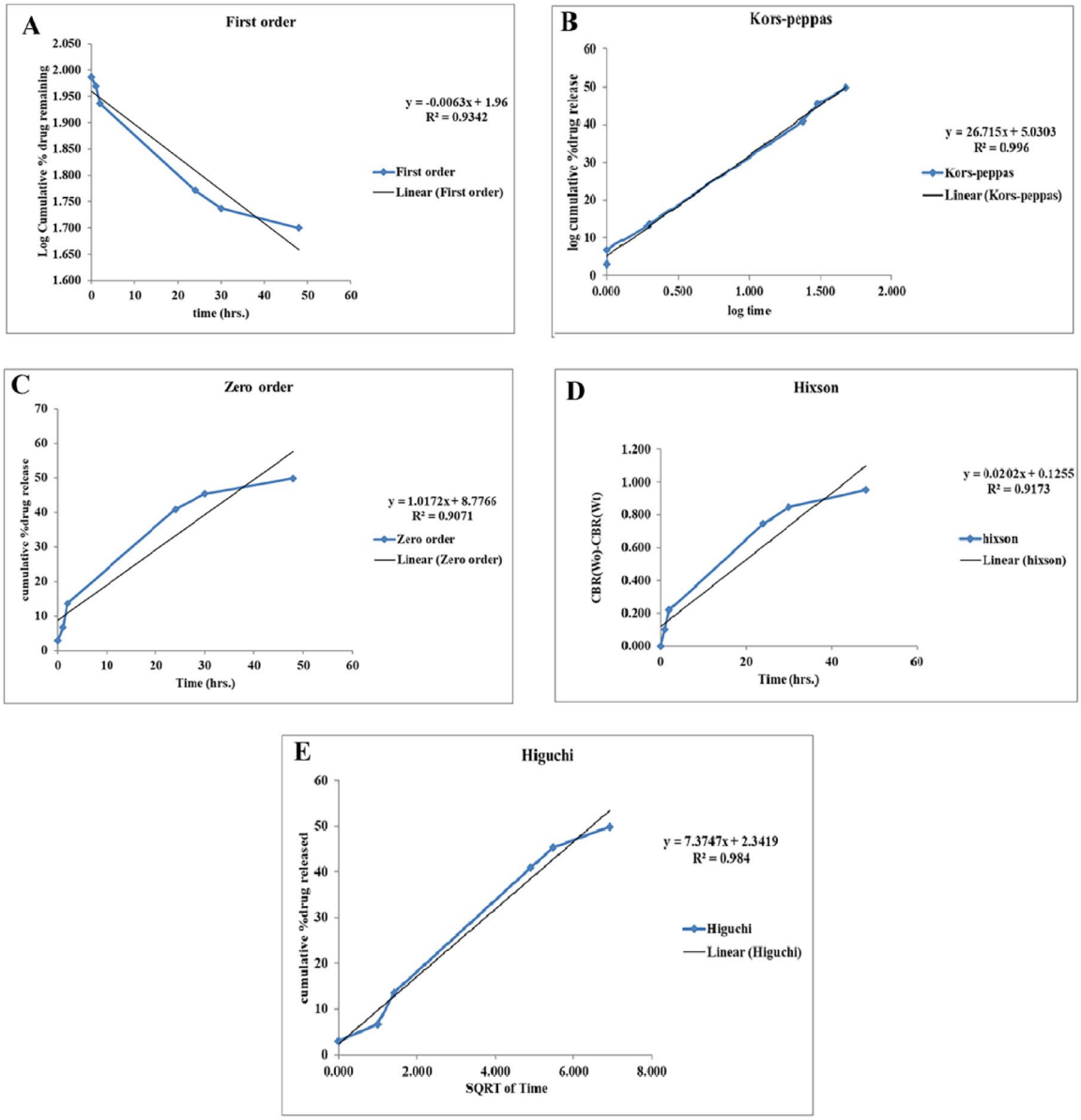

Fig. 5. The release kinetics of DNAzymes was analyzed using various mathematical models including (**A**) First-order kinetics with R^2 of 0.9342, (**B**) Korsmeyer-Peppas with R^2 of 0.996, (**C**) Zero-order kinetics with R^2 of 0.9071, (**D**) Hixson-Crowell with R^2 of 0.9173, and (**E**) Higuchi with R^2 of 0.984.

labeled DNZ-NLPs have diffused into the brain parenchyma, likely due to an increase in BBB permeability. The zoomed-in section (Fig. 9, B) reveals more detailed fluorescence patterns. These data suggest that under the in vivo experimental conditions, our nanoliposomes have a remarkable capability to pass through the BBB. These data, in corroboration with the rate of release, safety, and stability of DNZ-NLP in vitro (Figs. 5, 6, 7 and 8), demonstrated the effectiveness of nanoliposomes in delivering oligonucleotides in general and DNAzyme in particular to the brain.

Discussion

The BBB poses a significant impediment to drug delivery, with over 98% of pharmaceutical agents unable to efficiently traverse it, thereby diminishing their therapeutic efficacy in treating various neurological disorders, including neurodegenerative diseases[35]. To address this limitation, advanced nanotargeting technologies have emerged as a novel and promising strategy to enhance drug delivery and therapeutic impact at specific sites. These platforms facilitate the translocation of active drug compounds across the BBB either through encapsulation techniques or by functionalizing their surfaces with ligands specific to the BBB[36]. In particular, nanoliposomes stand out due to their high biocompatibility, biodegradability, and intrinsic ability to cross the

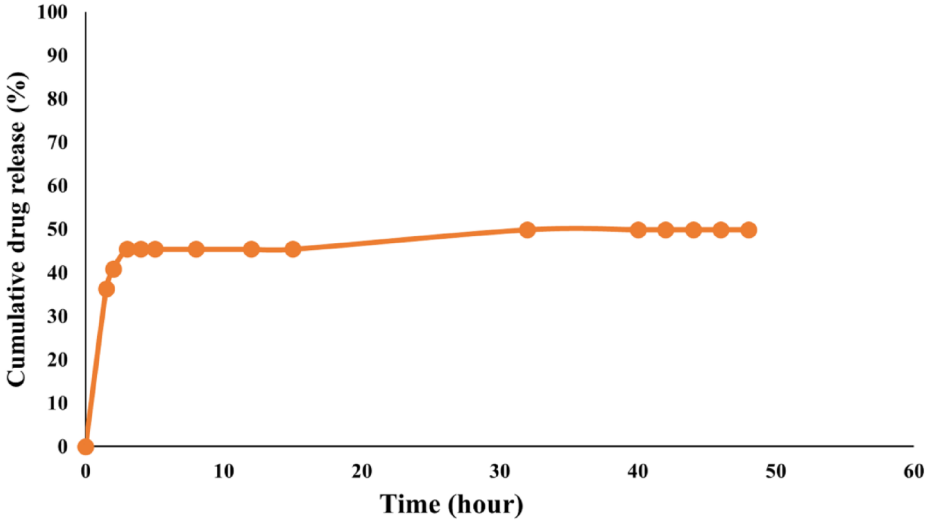

Fig. 6. The in vitro release of DNAzymes from nanoliposomes at a pH value of 7.4 over 48 h.

BBB, positioning them as a highly effective drug delivery platform with significant potential for applications in translational medicine[37].

In our study, we successfully designed a nanoliposomal drug delivery system capable of efficiently crossing the BBB. This innovative nanosystem encapsulates DNAzymes, a single-stranded catalytic DNA molecule renowned for its diverse biological functionalities, including gene silencing, the selective cleavage of specific mRNA sequences, and the facilitation of various chemical transformations through catalytic activity[38–40]. Moreover, DNAzymes have garnered considerable interest for their therapeutic potential in addressing a range of brain disorders, particularly neurodegenerative diseases[6]. The study incorporated DNAzymes into nanoliposomes to improve their ability to penetrate the BBB and reach cerebrovascular cells, thereby enhancing their therapeutic effectiveness for brain diseases.

In this study, DNZ-NLPs were fabricated using an ethanol injection method, which is a reproducible, rapid, and safe technique. This approach helped achieve an appropriate particle size and efficient DNAzyme encapsulation within the nanoliposomes[41].

The DLS and SEM analyses indicated that DNZ-NLPs displayed the desired morphology, with an average size of about 68 nm. This size was smaller than the 91.49 nm determined by the Zetasizer. The observed discrepancy in size measurements between DLS and SEM is common, primarily due to methodological differences; DLS determines the hydrodynamic diameter in solution, which includes the solvent layer surrounding the particles[42], whereas SEM evaluates particle size in the dry state[43]. SEM imaging offers greater precision in assessing surface morphology and size distribution[44,45]. The size of 68 nm is considered ideal for traversing the BBB[46]. Additionally, it is widely recognized that nanoparticles smaller than 500 nm can evade the reticuloendothelial system (RES), thereby prolonging their circulation time[47].

The DNZ-NLPs demonstrated a negative zeta potential of -12.6 mV at pH 7.4. The negative surface charge of the DNZ-NLPs underscores their robust stability and minimizes the likelihood of undesired clearance by the RES[48]. Negatively charged nanoparticles are known to elicit a lower immunological response compared to their positively or neutrally charged counterparts[49,50]. Notably, nanoparticles with a surface potential between −10 and +10 mV are less prone to nonspecific interactions and phagocytosis, enhancing their stability and bioavailability[51,52]. In comparison, B-NLPs displayed a less negative zeta potential of -8.42 mV. The reduction in negativity observed in B-NLPs can be attributed to the negative charge of phosphate groups in the DNAzyme backbone at physiological pH[53].

FTIR analysis demonstrated distinct spectral shifts indicative of interactions between DNAzyme molecules and phospholipid bilayers, thereby verifying the effective incorporation of DNAzymes into the liposomal structure. Furthermore, the results obtained from the dialysis method demonstrated an effective and controlled release profile of DNAzymes from nanoliposomes at pH 7.4, highlighting another advantageous characteristic of the newly developed DNZ-NLPs. This finding aligns with previous evidence suggesting that bilayer vesicles exhibit enhanced stability and controlled release properties for active compounds compared to unilamellar or multilamellar vesicles[54].

Furthermore, the MTT results showed no signs of cytotoxicity or cellular damage from the DNZ-NLPs on SH-SY5Y cells, even at high concentrations. This highlights the biocompatibility of the formulated DNZ-NLPs for brain cells. Our findings are consistent with previous research indicating that anionic nanoliposomes do not induce significant toxicity or damage to brain cells[55].

Fluorescence imaging confirmed effective uptake and targeted intracellular localization of DNZ-NLPs, with FITC and DAPI signals showing partial overlap, suggesting nuclear or perinuclear targeting. We hypothesized that the perinuclear localization significantly increases the effectiveness of DNAzyme therapy, making it a good agent for perinuclear mRNA scanning and targeting after emerging from the nuclei through nuclear pores[56].

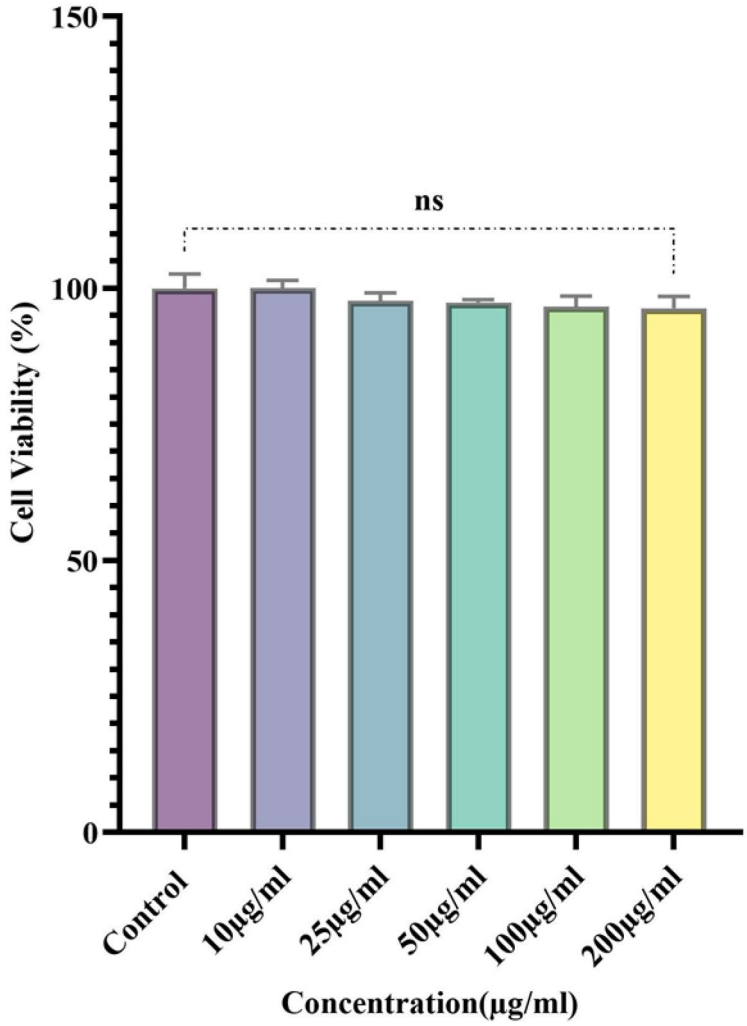

Fig. 7. Cell viability of the SH-SY5Y cells after treatment with 10, 25, 50, 100 and 200 μg/ml of DNZ-NLPs, indicating no cytotoxicity. Results were reported as mean ± SD (*$p \leq 0.1$, **$p \leq 0.01$, ***$p \leq 0.001$), in three independent replicates.

This co-localization points to a potential targeted mechanism, supporting future therapeutic or diagnostic applications and further studies on DNZ-NLP intracellular dynamics[57].

This study also demonstrated a significant increase in mouse brain fluorescence intensity for DNZ-NLPs (60%) compared to free DNAzymes (6%), indicating that nanoliposomes effectively transported DNAzymes across the BBB. This finding is particularly significant given the inherent challenges associated with drug delivery to the brain. The results highlight the considerable capability of the DNZ-NLPs to traverse the BBB, a feature that is critical for the development of therapeutic strategies aimed at neurodegenerative disorders such as HD, offering promising implications for the treatment of central nervous system diseases. The enhanced accumulation and prolonged retention observed in vivo further confirm the strong brain-penetrating capability of the nanoliposomes[13,58]. This permeability is likely dependent on specific physicochemical properties of the nanoliposomes, such as size, charge, and surface properties. Studies have revealed that upon reaching the BBB, nanoparticles can cross via several mechanisms, including carrier-mediated, receptor-mediated, and adsorptive-mediated transcytosis, as well as passive diffusion, clathrin-mediated endocytosis, and micropinocytosis[59]. Given the negative surface charge and absence of targeting ligands, our nanocarrier is unlikely to utilize receptor or adsorptive-mediated transcytosis. Instead, cellular uptake is expected to occur primarily through clathrin-mediated endocytosis and macropinocytosis, facilitated by its small size.

Although these findings represent a significant advancement in the field of nanomedicine and drug delivery systems, to enhance the robustness of the conclusions, future studies should incorporate quantitative analyses, such as fluorescence intensity measurements, co-localization studies, and statistical evaluations of BBB permeability across larger groups of samples. Furthermore, due to some limitations, the neuroprotective and neurotoxicity effects of DNZ-NLPs were not determined in mouse models. Therefore, more systematic researches

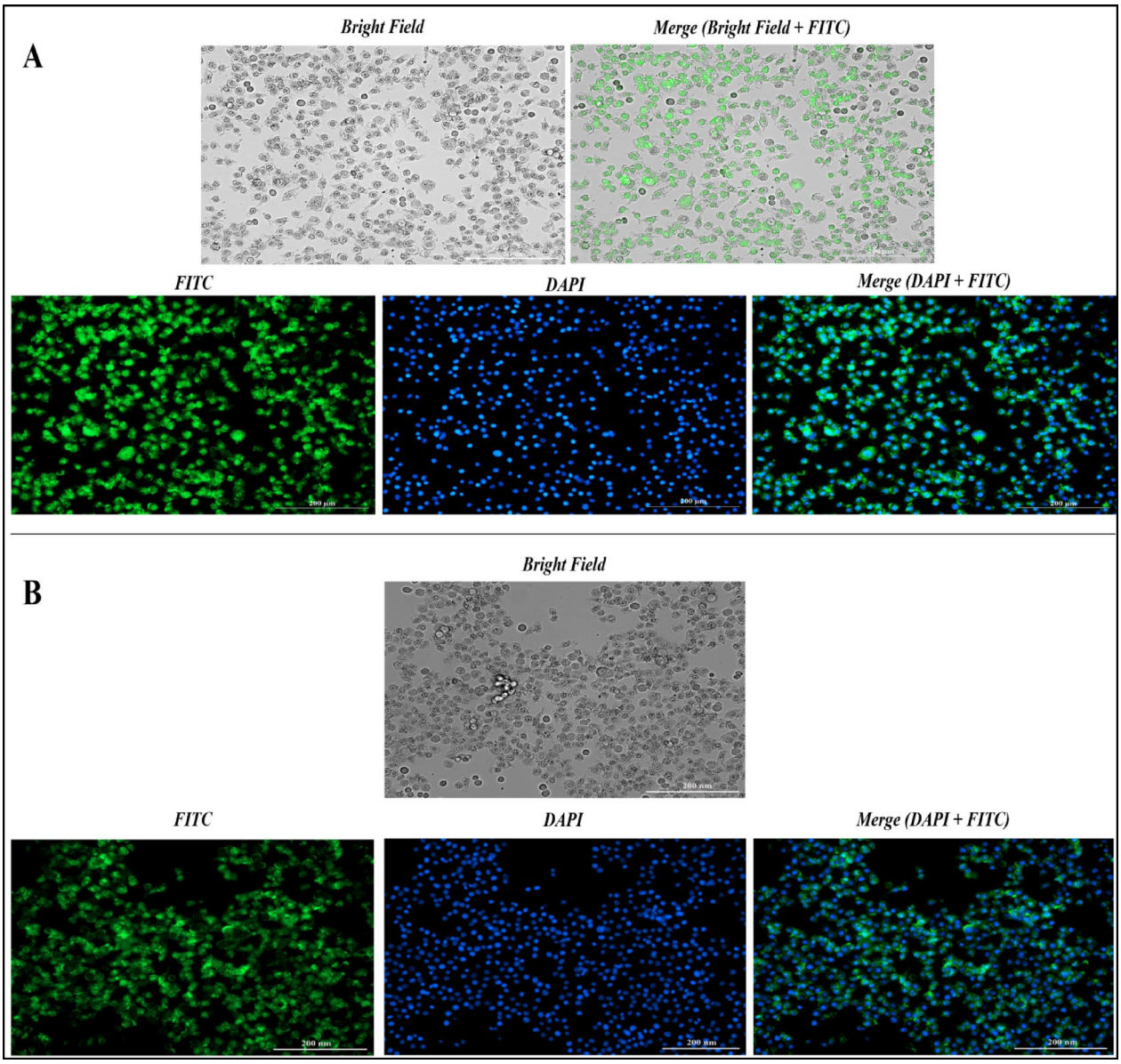

Fig. 8. Bright field, Bright field and FITC merged, FITC, DAPI and DAPI and FITC merged images of SH-SY5Y cells treated with (**A**) DNZ-NLPs and (**B**) DNAzyme, with a final concentration of 200 µg/mL at pH 7.4 with a 200 nm bar scale.

ranging from investigation of synaptic and postsynaptic markers to applying behavioral and serological tests are needed.

Conclusion

In this study, to explore the potential of nanoliposomes for targeted and controlled DNAzymes delivery in brain disorders therapy, DNZ-NLPs were successfully prepared, using the ethanol injection method. Our analysis of nanoliposomes and DNZ-NLPs confirmed their concern for suitable size, surface charge, and morphology, supporting their potential for effective brain drug delivery. Chemical and conformational analyses via FTIR further validated the successful DNAzyme encapsulation in nanoliposomes. The substantial drug release from nanoliposomes over 48 h highlights their effectiveness in controlled drug delivery. In vitro experiments revealed no cytotoxic effects of DNAzymes and DNZ-NLPs on SH-SY5Y cells even in high concentrations of 100 and 200 µg/mL, emphasizing the system's potential. Also, in vivo investigations confirmed the capability of DNZ-NLPs to effectively pass through the BBB in mouse models. This study represents the combination of DNZ-NLPs as a significant advancement in targeted brain drug delivery, highlighting natural lipid-based nanotechnology's role in the treatment of neurodegenerative diseases such as Huntington's disease (HD).

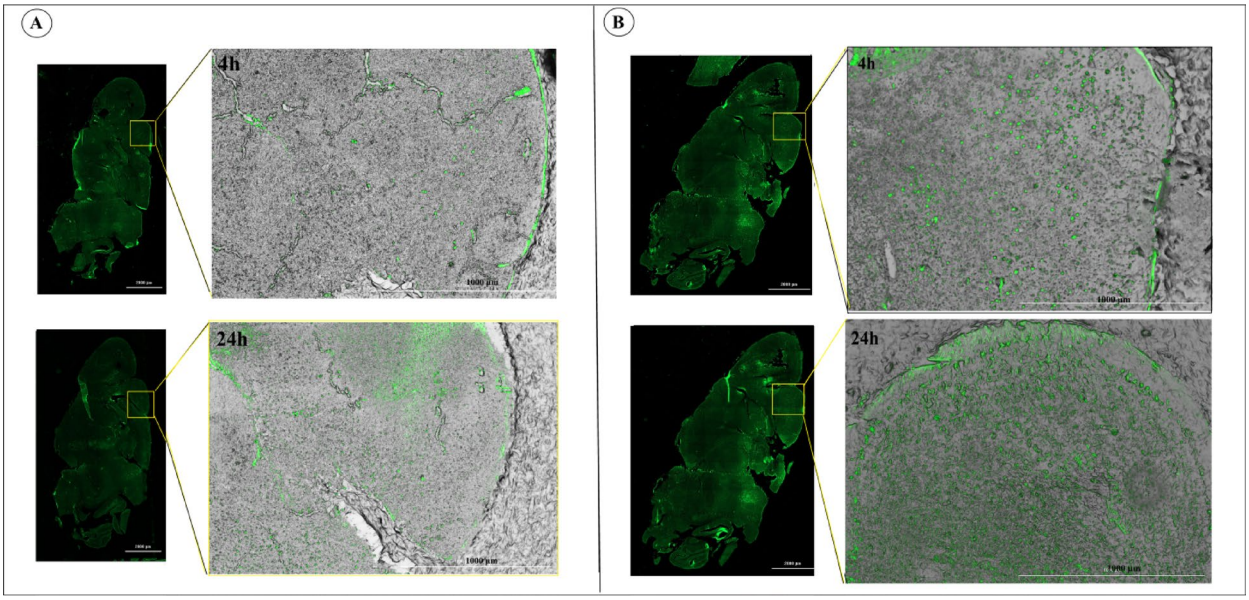

Fig. 9. UV microscopy results of mouse brains at (A) mice-brain tissue after being treated by free DNAzymes labeled FITC and (**B**) mice-brain tissue after being treated by DNZ-NLPs labeled FITC (X*1000 µm scales) at two times of 4 and 24 h after treatment.

Data availability

The data that support the findings of this study are listed in the article and are available from the corresponding author upon reasonable request. Contact: Faranak Aghaz: Nano Drug Delivery Research Center, Health Technology Institute, Kermanshah University of Medical Sciences, Kermanshah, Iran; Orcid.org/0000-0002-7311-4071; E-mail: Faranak_aghaz@yahoo.com.

Received: 19 March 2025; Accepted: 27 May 2025
Published online: 29 May 2025

References

1. Niazi, S. K. Non-Invasive Drug Delivery across the Blood-Brain Barrier: A Prospective Analysis. *Pharmaceutics* **15**, 2599 https://doi.org/10.3390/pharmaceutics15112599 (2023).
2. Zaib, S. et al. Neurodegenerative diseases: their onset, epidemiology, causes and treatment. *ChemistrySelect* **8**, e202300225 https://doi.org/10.1002/slct.202300225 (2023).
3. Hussain, M. S., Chaturvedi, V., Goyal, S., Singh, S. & Mir, R. H. J. C. B. C. An update on the application of nano phytomedicine as an emerging therapeutic tool for neurodegenerative diseases. *Curr. Bioact Compd.* **20**, 78–91. https://doi.org/10.2174/0115734072258656231013085318 (2024).
4. Patra, J. K. et al. Nano based drug delivery systems: recent developments and future prospects. *J. Nanobiotechnol.* **16**, 1–33. https://doi.org/10.1186/s12951-018-0392-8 (2018).
5. O'Connor, D. M. & Boulis, N. M. Gene therapy for neurodegenerative diseases. *Trends Mol. Med.* **21**, 504–512. https://doi.org/10.1016/j.molmed.2015.06.001 (2015).
6. Zhang, N. et al. DNAzyme cleavage of CAG repeat RNA in polyglutamine diseases. *Neurother* **18**, 1710–1728. https://doi.org/10.1007/s13311-021-01075-w (2021).
7. Khachigian, L. M. Catalytic DNAs as potential therapeutic agents and sequence-specific molecular tools to dissect biological function. *J. Clin. Invest.* **106**, 1189–1195. https://doi.org/10.1172/jci11620 (2000).
8. Abdelgany, A., Ealing, J., Wood, M. & Beeson, D. Selective DNAzyme-mediated cleavage of achr mutant transcripts by targeting the mutation site or through mismatches in the binding arm. *J. RNAi Gene Silencing.* **1**, 32–37 (2005). https://pmc.ncbi.nlm.nih.gov/articles/PMC2737196/
9. Chakravarthy, M., Aung-Htut, M. T., Le, B. T. & Veedu, R. N. Novel Chemically-modified DNAzyme targeting integrin alpha-4 RNA transcript as a potential molecule to reduce inflammation in multiple sclerosis. *Sci. Rep.* **7**, 1613. https://doi.org/10.1038/s41598-017-01559-w (2017).
10. Fokina, A. A., Stetsenko, D. A. & François, J. C. DNA enzymes as potential therapeutics: towards clinical application of 10–23 dnazymes. *Expert Opin. Biol. Ther.* **15**, 689–711. https://doi.org/10.1517/14712598.2015.1025048 (2015).
11. Cho, E. A. et al. Safety and tolerability of an intratumorally injected DNAzyme, Dz13, in patients with nodular basal-cell carcinoma: a phase 1 first-in-human trial (DISCOVER). *Lancet* **381**, 1835–1843. https://doi.org/10.1016/S0140-6736(12)62166-7 (2013).
12. Hallett, M. A., Dalal, P., Sweatman, T. W. & Pourmotabbed, T. The distribution, clearance, and safety of an anti-MMP-9 DNAzyme in normal and MMTV-PyMT Transgenic mice. *Nucleic Acid Ther.* **23**, 379–388. https://doi.org/10.1089/nat.2012.0348 (2013).
13. Schubert, S. et al. RNA cleaving '10–23' dnazymes with enhanced stability and activity. *Nucleic Acids Res.* **31**, 5982–5992. https://doi.org/10.1093/nar/gkg791 (2003).
14. Naqvi, S., Panghal, A., Flora, S. J. S. & Nanotechnology A promising approach for delivery of neuroprotective drugs. *Front. Neurosci.* **14** https://doi.org/10.3389/fnins.2020.00494 (2020).
15. Dhiman, N., Awasthi, R., Sharma, B., Kharkwal, H. & Kulkarni, G. T. Lipid nanoparticles as carriers for bioactive delivery. *Front. Chem.* **9** https://doi.org/10.3389/fchem.2021.580118 (2021).
16. Haider, M., Abdin, S. M., Kamal, L. & Orive, G. Nanostructured Lipid Carriers for Delivery of Chemotherapeutics: A Review. *Pharmaceutics* **12**, https://doi.org/10.3390/pharmaceutics12030288 (2020).

17. Duan, Y. et al. A brief review on solid lipid nanoparticles: part and parcel of contemporary drug delivery systems. *RSC Adv.* **10**, 26777–26791. https://doi.org/10.1039/D0RA03491F (2020).
18. Salunkhe, S. S., Bhatia, N. M. & Bhatia, M. S. Implications of formulation design on lipid-based nanostructured carrier system for drug delivery to brain. *Drug Deliv.* **23**, 1306–1316. https://doi.org/10.3109/10717544.2014.943337 (2016).
19. Costa, C. P., Moreira, J. N., Lobo, S., Silva, A. C. & J. M. & Intranasal delivery of nanostructured lipid carriers, solid lipid nanoparticles and nanoemulsions: A current overview of in vivo studies. *Acta Pharm. Sin B.* **11**, 925–940. https://doi.org/10.1016/j.apsb.2021.02.012 (2021).
20. Costa, C. P. et al. In vitro studies on nasal formulations of nanostructured lipid carriers (NLC) and solid lipid nanoparticles (SLN). *Pharmaceuticals (Basel).* **14** https://doi.org/10.3390/ph14080711 (2021).
21. Costa, C., Moreira, J. N., Amaral, M. H., Lobo, S., Silva, A. C. & J. M. & Nose-to-brain delivery of lipid-based nanosystems for epileptic seizures and anxiety crisis. *J. Control Release.* **295**, 187–200. https://doi.org/10.1016/j.jconrel.2018.12.049 (2019).
22. Satapathy, M. K. et al. Solid Lipid Nanoparticles (SLNs): An Advanced Drug Delivery System Targeting Brain through BBB. *Pharmaceutics* **13**, https://doi.org/10.3390/pharmaceutics13081183 (2021).
23. Zhang, Z. et al. Brain-targeted drug delivery by manipulating protein Corona functions. *Nat. Commun.* **10** https://doi.org/10.1038/s41467-019-11593-z (2019).
24. Zhang, Y. et al. Brain-targeted delivery of obidoxime, using aptamer-modified liposomes, for detoxification of organophosphorus compounds. *J. Control Release.* **329**, 1117–1128. https://doi.org/10.1016/j.jconrel.2020.10.039 (2021).
25. Pons, M., Foradada, M. & Estelrich, J. Liposomes obtained by the ethanol injection method. *Int. J. Pharm.* **95**, 51–56. https://doi.org/10.1016/0378-5173(93)90389-W (1993).
26. Akbari, B., Tavandashti, M. & Zandrahimi, M. Particle size characterization of nanoparticles- a practicalapproach. *Iran. J. MATER. SCI. ENG.* **8**, 48–56 (2011). https://ijmse.iust.ac.ir/article-1-341-en.html
27. Lv, Y. et al. Visual validation of the measurement of entrapment efficiency of drug nanocarriers. *Int. J. Pharm.* **547**, 395–403. https://doi.org/10.1016/j.ijpharm.2018.06.025 (2018).
28. Akbari, J. et al. The design of Naproxen solid lipid nanoparticles to target skin layers. *Colloids Surf. B Biointerfaces.* **145**, 626–633. https://doi.org/10.1016/j.colsurfb.2016.05.064 (2016).
29. D'Souza, S. A. Review of In Vitro Drug Release Test Methods for Nano-Sized Dosage Forms. *Adv. Pharm.* **2014**, 304757, https://doi.org/10.1155/2014/304757 (2014).
30. Tian, J. et al. Nanoliposomal formulation encapsulating celecoxib and genistein inhibiting COX-2 pathway and Glut-1 receptors to prevent prostate cancer cell proliferation. *Cancer Lett.* **448**, 1–10. https://doi.org/10.1016/j.canlet.2019.01.002 (2019).
31. Feles, S. et al. Streamlining culture conditions for the neuroblastoma cell line SH-SY5Y: A prerequisite for functional studies. *Methods Protoc.* **5**, 58. https://doi.org/10.3390/mps5040058 (2022).
32. Mihanfar, A. et al. Doxorubicin loaded magnetism nanoparticles based on cyclodextrin dendritic-graphene oxide inhibited MCF-7 cell proliferation. *Biomol. Concepts.* **12**, 8–15. https://doi.org/10.1515/bmc-2021-0002 (2021).
33. Hassan, U. A., Hussein, M. Z., Alitheen, N. B., Ariff, Y., Masarudin, M. J. & S. A. & In vitro cellular localization and efficient accumulation of fluorescently tagged biomaterials from monodispersed Chitosan nanoparticles for Elucidation of controlled release pathways for drug delivery systems. *Int. J. Nanomed.* **13**, 5075–5095. https://doi.org/10.2147/ijn.s164843 (2018).
34. Abedi Gaballu, F. et al. Comparative of in-vitro evaluation between erlotinib loaded nanostructured lipid carriers and liposomes against A549 lung Cancer cell line. *Iran. J. Pharm. Res.* **18**, 1168–1179. https://doi.org/10.22037/ijpr.2019.1100775 (2019).
35. Wu, C. et al. Preparation and pharmacokinetics of Brain-Targeted nanoliposome loaded with Rutin. *Int. J. Mol. Sci.* **25**, 11404. https://doi.org/10.3390/ijms252111404 (2024).
36. Zhou, X., Smith, Q. R. & Liu, X. Brain penetrating peptides and peptide-drug conjugates to overcome the blood-brain barrier and target CNS diseases. *Wiley Interdiscip Rev. Nanomed. Nanobiotechnol.* **13**, e1695. https://doi.org/10.1002/wnan.1695 (2021).
37. Susa, F., Arpicco, S., Pirri, C. F. & Limongi, T. An overview on the physiopathology of the Blood–Brain barrier and the Lipid-Based nanocarriers for central nervous system delivery. *Pharmaceutics* **16**, 849. https://doi.org/10.3390/pharmaceutics16070849 (2024).
38. Peracchi, A. DNA catalysis: potential, limitations, open questions. *Chembiochem* **6**, 1316–1322. https://doi.org/10.1002/cbic.200500098 (2005).
39. Dass, C. R., Choong, P. F. & Khachigian, L. M. DNAzyme technology and cancer therapy: cleave and let die. *Mol. Cancer Ther.* **7**, 243–251. https://doi.org/10.1158/1535-7163.mct-07-0510 (2008).
40. Wang, F., Saran, R. & Liu, J. Tandem dnazymes for mRNA cleavage: choice of enzyme, metal ions and the antisense effect. *Bioorg. Med. Chem. Lett.* **25**, 1460–1463. https://doi.org/10.1016/j.bmcl.2015.02.032 (2015).
41. Lombardo, D. & Kiselev, M. A. Methods of liposomes preparation: formation and control factors of versatile nanocarriers for biomedical and nanomedicine application. *Pharmaceutics* **14**, 543. https://doi.org/10.3390/pharmaceutics14030543 (2022).
42. Maguire, C. M., Rösslein, M., Wick, P. & Prina-Mello, A. Characterisation of particles in solution - a perspective on light scattering and comparative technologies. *Sci. Technol. Adv. Mater.* **19**, 732–745. https://doi.org/10.1080/14686996.2018.1517587 (2018).
43. Liu, M. et al. Luminescence tunable fluorescent organic nanoparticles from polyethyleneimine and maltose: facile Preparation and bioimaging applications. *RSC Adv.* **4**, 22294–22298. https://doi.org/10.1039/C4RA03103B (2014).
44. Aghaz, F. et al. Co-encapsulation of tertinoin and Resveratrol by solid lipid nanocarrier (SLN) improves mice in vitro matured oocyte/ morula-compact stage embryo development. *Theriogenology* **171**, 1–13. https://doi.org/10.1016/j.theriogenology.2021.05.007 (2021).
45. Motiei, M. & Kashanian, S. Novel amphiphilic Chitosan nanocarriers for sustained oral delivery of hydrophobic drugs. *Eur. J. Pharm. Sci.* **99**, 285–291. https://doi.org/10.1016/j.ejps.2016.12.035 (2017).
46. Patra, J. K. et al. Nano based drug delivery systems: recent developments and future prospects. *J. Nanobiotechnol.* **16**, 71. https://doi.org/10.1186/s12951-018-0392-8 (2018).
47. Kommareddy, S. & Amiji, M. Poly(ethylene glycol)-modified thiolated gelatin nanoparticles for glutathione-responsive intracellular DNA delivery. *Nanomedicine* **3**, 32–42. https://doi.org/10.1016/j.nano.2006.11.005 (2007).
48. Xiao, K. et al. The effect of surface charge on in vivo biodistribution of PEG-oligocholic acid based micellar nanoparticles. *Biomaterials* **32**, 3435–3446. https://doi.org/10.1016/j.biomaterials.2011.01.021 (2011).
49. Liu, J., Zhang, R. & Xu, Z. P. Nanoparticle-Based nanomedicines to promote Cancer immunotherapy: recent advances and future directions. *Small* **15**, e1900262. https://doi.org/10.1002/smll.201900262 (2019).
50. Arvizo, R. R. et al. Modulating pharmacokinetics, tumor uptake and biodistribution by engineered nanoparticles. *PLoS One* **6**, e24374, https://doi.org/10.1371/journal.pone.0024374 (2011).
51. Ernsting, M. J., Murakami, M., Roy, A. & Li, S. D. Factors controlling the pharmacokinetics, biodistribution and intratumoral penetration of nanoparticles. *J. Control Release.* **172**, 782–794. https://doi.org/10.1016/j.jconrel.2013.09.013 (2013).
52. Bhatia, S. in *Natural Polymer Drug Delivery Systems: Nanoparticles, Plants, and Algae* (ed Saurabh Bhatia) 33–93 (Springer International Publishing, 2016). https://doi.org/10.1007/978-3-319-41129-3
53. Nakano, S., Horita, M., Kobayashi, M. & Sugimoto, N. Catalytic activities of ribozymes and dnazymes in water and mixed aqueous media. *Catalysts* **7**, 355. https://doi.org/10.3390/catal7120355 (2017).
54. Li, W. et al. Development and physicochemical characterization of nanoliposomes with incorporated oleocanthal, Oleacein, Oleuropein and Hydroxytyrosol. *Food Chem.* **384**, 132470. https://doi.org/10.1016/j.foodchem.2022.132470 (2022).
55. Momtazi-Borojeni, A. A., Hatamipour, M., Sarborji, M. R., Jaafari, M. R. & Sahebkar, A. Preclinical toxicity assessment of anionic nanoliposomes. *Adv. Ind. Eng. Polym. Res.* **7**, 144–150. https://doi.org/10.1016/j.aiepr.2022.11.002 (2024).

56. Saroufim, M. A. et al. The nuclear basket mediates perinuclear mRNA scanning in budding yeast. *J. Cell. Biol.* **211**, 1131–1140. https://doi.org/10.1083/jcb.201503070 (2015).
57. Zhao, F. et al. Cellular uptake, intracellular trafficking, and cytotoxicity of nanomaterials. *Small* **7**, 1322–1337. https://doi.org/10.1002/smll.201100001 (2011).
58. Vieira, D. B. & Gamarra, L. F. Getting into the brain: liposome-based strategies for effective drug delivery across the blood-brain barrier. *Int. J. Nanomed.* **11**, 5381–5414. https://doi.org/10.2147/ijn.s117210 (2016).
59. Cai, X., Drummond, C. J., Zhai, J. & Tran, N. Lipid nanoparticles: versatile drug delivery vehicles for traversing the blood brain barrier to treat brain Cancer. *Adv. Funct. Mater.* **34**, 2404234. https://doi.org/10.1002/adfm.202404234 (2024).

Acknowledgements

The authors have no conflict of interest to disclose.Hi dear editor of Scientific ReportsYes, we have confirmed that "Figure 1" was drawn by our team, drawn by one of my co-authors listed in the authors list.Manuscript Title: Facilitating DNAzyme Transport Across the Blood-Brain Barrier with Nanoliposome TechnologyManuscript ID: ab07b083-96c7-45b2-bb3b-8580a22ebe6e v2.0.

Author contributions

F.A., writing–review, and editing; M. H. and, Z. A. writing–original draft; P. A., E. A., S. E.N, A. P., and T. P. methodology; S. S., A. S. S., S. M. G., W. S. D., and J. T. M. investigation; S. S., Y. Y., formal analysis; G. B., and Z. A. conceptualization; F. A. and T. P. supervision; F. (A) and G. (B) funding acquisition. All authors reviewed the manuscript.

Funding

This study was financially supported by Kermanshah University of Medical Sciences (IR.KUMS.AEC.1401.042). And we confirmed the study is reported under ARRIVE guidelines.

Declarations

Competing interests

The authors declare no competing interests.

Additional information

Correspondence and requests for materials should be addressed to F.A. or T.P.

Reprints and permissions information is available at www.nature.com/reprints.

Publisher's note Springer Nature remains neutral with regard to jurisdictional claims in published maps and institutional affiliations.